

Experimental performance assessment of mantis 2, hybrid leg-wheel mobile robot

Original

Experimental performance assessment of mantis 2, hybrid leg-wheel mobile robot / Bruzzone, L., Fanghella, P., Quaglia, G.. - In: INTERNATIONAL JOURNAL OF AUTOMATION TECHNOLOGY. - ISSN 1881-7629. - STAMPA. - 11:3(2017), pp. 396-403. [10.20965/ijat.2017.p0396]

Availability:

This version is available at: 11583/2674739 since: 2017-06-16T19:34:41Z

Publisher:

Fuji Technology Press

Published

DOI:10.20965/ijat.2017.p0396

Terms of use:

This article is made available under terms and conditions as specified in the corresponding bibliographic description in the repository

Publisher copyright

(Article begins on next page)

Paper:

Experimental Performance Assessment of Mantis 2, Hybrid Leg-Wheel Mobile Robot

Luca Bruzzone^{*,†}, Pietro Fanghella^{*}, and Giuseppe Quaglia^{**}

^{*}DIME, University of Genoa

Via Opera Pia 15A, 16145 Genoa, Italy

[†]Corresponding author, E-mail: bruzzone@dimec.unige.it

^{**}DIMEAS, Polytechnic University of Turin, Torino, Italy

[Received September 27, 2016; accepted November 11, 2016]

Mantis 2 is a small-scale leg-wheel ground mobile robot, designed for exploration, surveillance and inspection tasks in unstructured environments. It is equipped with two actuated front wheels, two passive rear wheels, and two rotating legs with praying Mantis profile, specially conceived for step and obstacle climbing. Locomotion is purely wheeled on regular surfaces, with high energetic efficiency and maneuverability, and with stable camera vision. In case of obstacles or terrain irregularities, the rotating legs increase the motion capability. The main innovation of the second version is the introduction of passive one-way auxiliary wheels on each leg, which improve the efficacy of step climbing. The paper discusses analytical and experimental results on step ascent and descent and locomotion on irregular surfaces.

Keywords: hybrid leg-wheel locomotion, ground mobile robot, step climbing

1. Introduction

The importance of service robotics has been continuously increasing over the last few years. While the application of robots in structured industrial environments is well consolidated and mature, the adoption of robots for intervention in unstructured environments (terrestrial [1, 2], aerial [3, 4] and underwater [5, 6]) is still at an early stage. In particular, ground mobile robots can be applied to a wide range of tasks, in order to replace direct human involvement in dangerous locations, or simply to reduce operational costs. Small-scale ground mobile robots can move in narrow spaces, and in the presence of radioactive or chemical contamination.

For all these reasons, the development of surveillance, inspection, and homeland security ground mobile robots is today a fundamental research area, which involves not only mechatronic aspects but also obstacle detection, scene recognition, and artificial intelligence [7–9].

Independent of the specific task, which determines its on-board equipment, a ground mobile robot is primarily characterized by its locomotion principle. There are three

main classes of robotic locomotion systems: wheeled (W), legged (L) and tracked (T), and four possible hybrid combinations (LW, LT, LW, LWT). Other locomotion principles (e.g., slithering, adhesive, snake-like robots) are not general-purpose and are oriented toward specific applications.

A locomotion system for surveillance mobile robots must provide motion capability in indoor and outdoor unstructured requirements, high energetic efficiency, maneuverability in narrow spaces, and stable camera vision. The advantages and disadvantages of different locomotion approaches are discussed in [10–12]. In general, locomotion systems with wheels (W, LW, WT, LWT) maximize energetic efficiency and speed on regular and compact surfaces, while locomotion systems including legs (L, LW, LT, LWT) maximize obstacle crossing capability and operative flexibility. Tracks are particularly efficient on soft and yielding terrains.

One of the basic parameters for selecting the locomotion approach is the size of the robot. For medium to large robots, the inertial forces acting during locomotion are never negligible; therefore, locomotion principles characterized by strong trajectory discontinuities and shocks are not suitable. Consequently, legged locomotion for big robots is necessarily characterized by high mechanical and control complexity.

On the contrary, for small-scale robots, the inertial forces are less critical, and simplified hybrid locomotion mechanisms can be adopted, conjugating the benefits of legs and wheels without significantly increasing the complexity and costs. Examples are rotating legged robots [13–15] and stepping-triple-wheel robots [16–18], characterized by locomotion units with three legs placed at 120°, with a wheel at each end. Another approach to implement hybrid leg-wheel locomotion is the adoption of legs with outer circular profile, which can act as wheels when properly coordinated [19–21].

Mantis belongs to this category of small-scale ground robots, suitable for surveillance and inspection tasks. It is a hybrid robot with four wheels, two independently actuated and two idle, and two legs. The first version of Mantis and its main features are presented in [22]; the step-climbing maneuver, based on the praying mantis leg shape, is analyzed by multibody simulation in [23,

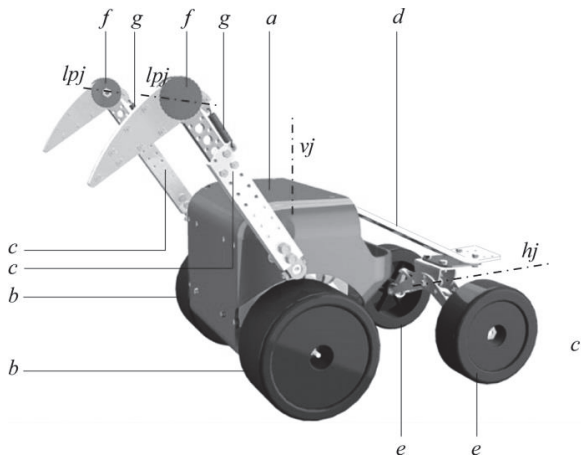


Fig. 1. Mantis 2 main components.

24]; the benefits of the introduction of one-way auxiliary wheels on the legs are shown by multibody simulation in [25]. The present paper is organized as follows: Section 2 describes the Mantis 2 architecture, with auxiliary wheels and variable-length legs; Section 3 discusses the influence of the main geometrical parameters on the stability in step ascent and descent; Section 4 presents experimental results on hybrid locomotion capability with variable leg length; and Section 5 provides the conclusions of the study.

2. Mantis 2 Architecture

Mantis 2 is a general-purpose ground mobile robot with a maximum payload of 1 kg, suitable for surveillance tasks. Its overall dimensions are approximately $350 \times 300 \times 200$ mm. The main body (**Fig. 1**, *a*) is equipped with two independently actuated wheels (*b*) and two independently actuated praying mantis legs (*c*). In the second version of the Mantis, each leg is variable-length and is connected to an auxiliary wheel (*f*) by a one-way bearing; the tip of the leg is connected to the rest of the leg by a passive revolute joint (*lpj*), and can bend internally to soften impacts during obstacle descent, exploiting the elastic return force of the spring (*g*).

The rear axle (*d*) is characterized by two idle wheels (*e*) and two passive revolute joints (*hj* and *vj*) to adapt to uneven ground.

Figure 2 shows the step climbing sequence: the robot approaches the step (**Fig. 2**, *a*), then the legs grasp the step upper surface to lift up the robot body (**Fig. 2**, *b – c*). When the legs stop, as the center of gravity of the robot is further forward than the leg to ground contact point, the robot rotates forward until the front wheels touch the ground (**Fig. 2**, *d*). Then the legs rotate backward to lift up the rear axle (**Fig. 2**, *e*); when the rear axle is sufficiently high, the front wheels move the robot forward to complete the maneuver (**Fig. 2**, *f*).

In the first version of the Mantis, without unidirectional auxiliary wheels on the leg extremities, the last phase

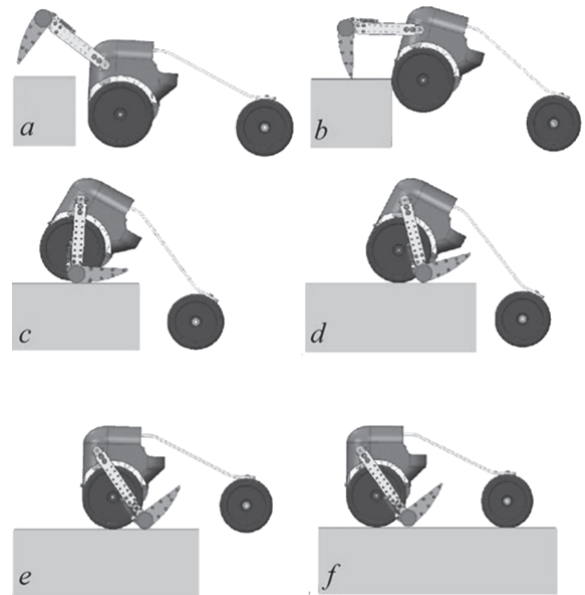


Fig. 2. Step climbing sequence.

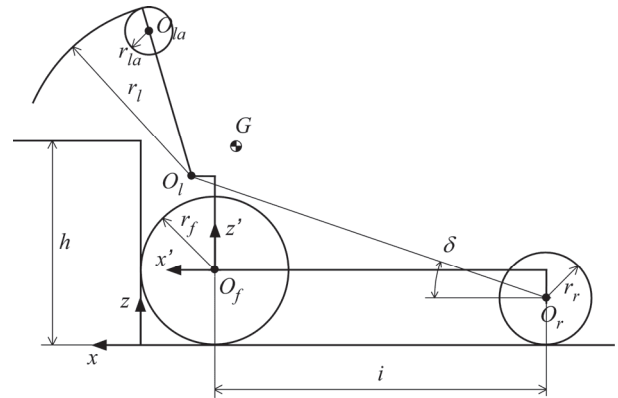


Fig. 3. Main geometrical parameters.

(horizontal motion with lifted rear axle) was the most critical: this topic is discussed analytically and by multibody simulation in [25]. The auxiliary wheels are connected to the legs by one-way bearings, so they can rotate forward during step climbing, reducing friction between legs and ground, but they cannot rotate backward during hybrid leg-wheel locomotion on irregular terrains, avoiding the consequent traction reduction.

The main geometrical parameters of the robot (**Fig. 3**) are collected in **Table 1**. The robot reference frame is (x', z') , with its origin on the front wheel axis O_f . For the sake of generality, the static analysis is performed using the nondimensional ratios of **Table 2**.

Table 2 also shows the base values of the geometrical ratios for the Mantis 2 prototype. In the following, the effects of varying some of these ratios will be analytically and experimentally discussed; in absence of different indications, the base values are assumed for the remaining geometrical ratios.

Mantis' maximum speed is 2.3 km/h on flat ground;

Table 1. Main geometrical parameters.

Parameter	Symbol	Value
front wheel radius	r_f	55 mm
rear wheel radius	r_r	45 mm
leg radius	r_l	163 mm
auxiliary wheel radius	r_{la}	15 mm
x-coordinate of O_l in the robot ref. frame	x'_l	32 mm
z-coordinate of O_l in the robot ref. frame	z'_l	80 mm
wheelbase	i	239 mm
step height	h	160 mm

Table 2. Main geometrical ratios.

Ratio symbol	Definition	Base value
α	$2r_f/h$	0.69
β	r_r/r_f	0.82
γ	i/r_f	4.35
ξ_l	x'_l/r_f	0.58
ψ_l	z'_l/r_f	1.45
γ_l	r_l/r_f	2.96

it climbs slopes up to 71.5% (35.6°) with static friction coefficient between front wheels and terrain greater than or equal to 0.77.

3. Stability Analysis in Step Climbing

3.1. Stability in Step Ascent

Step climbing is performed by Mantis at low speed, in quasi-static conditions; therefore stability can be analyzed statically with good approximation, considering the maximum pitch angle position represented in **Fig. 4**. The position of the overall center of mass (COM) G is represented nondimensionally by the ratios $\xi_G = x'_G/r_f$ and $\psi_G = z'_G/r_f$, where x'_G and z'_G are the COM coordinates in the robot frame. The angle $\lambda_{G,asc}$ is the angle between the segment $G - O_r$ and the vertical direction (O_r is the rear wheel axis point in the $x - z$ plane) in the maximum pitch position shown in **Fig. 4** for a considered nondimensional step height ($1/\alpha$). Considering the angles φ_{asc} , θ_{asc} and δ_G shown in the geometrical model of **Fig. 4**, the angle $\lambda_{G,asc}$ can be expressed by the following equation:

$$\begin{aligned} \lambda_{G,asc} &= \frac{\pi}{2} - \theta_{asc} - \delta_G = \frac{\pi}{2} - (\varphi_{asc} - \delta) - \delta_G \\ &= \frac{\pi}{2} - \arcsin\left(\frac{\gamma_l + \frac{2}{\alpha} - \beta}{\sqrt{(\gamma + \xi_l)^2 + (\psi_l + 1 - \beta)^2}}\right) \\ &\quad + \arctan\left(\frac{\psi_l + 1 - \beta}{\gamma + \xi_l}\right) - \arctan\left(\frac{\psi_G + 1 - \beta}{\gamma + \xi_G}\right) \end{aligned} \quad (1)$$

The static stability condition is verified if the vertical projection of G lies between the vertical projections of O_l and O_r ($x_G < x_{Ol}$ and $x_G > x_{Or}$). With reasonable mass

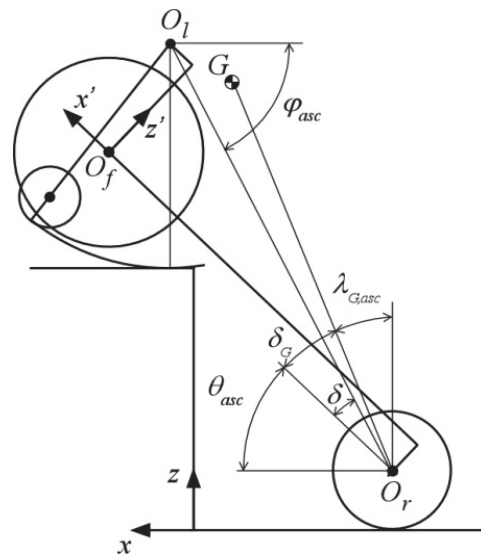


Fig. 4. Stability in step ascent (maximum pitch position).

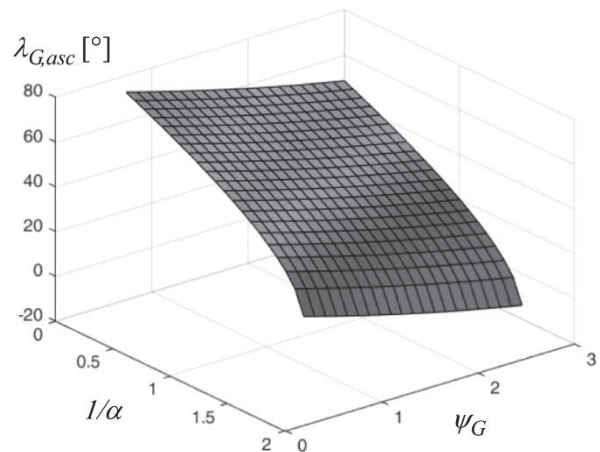


Fig. 5. $\lambda_{G,asc}$ as a function of $1/\alpha$ and ψ_G .

distributions the first condition is always verified, otherwise the robot is unstable even on horizontal ground; the second condition is verified if and only if $\lambda_{G,asc}$ is greater than zero.

One of the most important parameters for robot stability is the position of the COM, which varies if a payload is fixed above the robot's main body; without payload the COM nondimensional coordinates are $\xi_G = 0$, $\psi_G = 0.73$. The 3D graph in **Fig. 5** shows the influence of the COM vertical coordinate (ψ_G) and of the step height ($1/\alpha$) on the angle $\lambda_{G,asc}$, with ξ_G always null (with payloads fixed on the top of the main body, this hypothesis is rather a good approximation). Obviously, higher steps (higher $1/\alpha$) and higher payloads (higher ψ_G) are critical for the robot stability.

The 3D graph of **Fig. 6** shows the influence of the leg length (γ_l), which is variable on Mantis 2: longer legs decrease stability during step climbing, because the maximum pitch angle increases. On the other hand, a lower

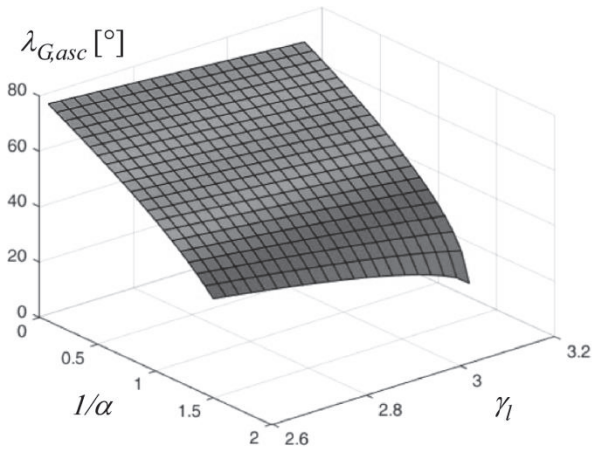


Fig. 6. $\lambda_{G,asc}$ as a function of $1/\alpha$ and γ_l .

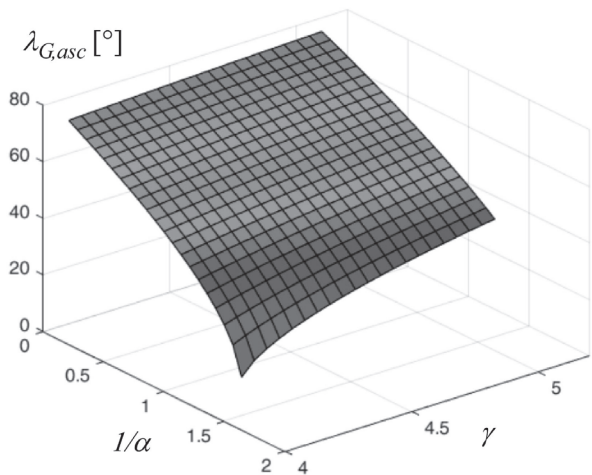


Fig. 7. $\lambda_{G,asc}$ as a function of $1/\alpha$ and γ .

limit of the leg length is imposed by the requirement of touching the ground during hybrid locomotion, as discussed in Section 4.

Figure 7 shows the influence of the wheelbase (γ): for the same step height, a longer wheelbase decreases the pitch angle and increases stability. Nevertheless, excessive values of the wheelbase limit the robot agility and maneuverability in narrow spaces, where the robot can pivot around a vertical axis, with opposite speeds of the front wheels. To avoid excessive encumbrance of the rear axle, an appropriate upper limit for γ is approximately 5.

3.2. Stability in Step Descent

Stability in step descent can be assessed by considering the geometry of **Fig. 8**, which leads to the following expression:

$$\lambda_{G,desc} = \arctan\left(\frac{N_1}{D_1}\right)$$

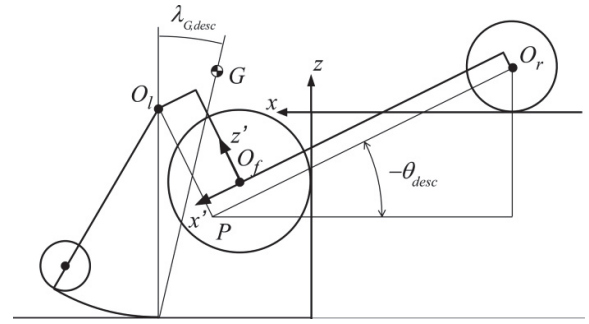


Fig. 8. Stability in step descent.

$$\begin{aligned} N_1 &= \psi_l \sin(-\theta_{desc}) + \xi_l \cos(-\theta_{desc}) \\ &\quad - \psi_G \sin(-\theta_{desc}) - \xi_G \cos(-\theta_{desc}) \\ D_1 &= \beta - \gamma \sin(-\theta_{desc}) \\ &\quad + (1 - \beta + \psi_G) \cos(-\theta_{desc}) + \\ &\quad - \xi_G \sin(-\theta_{desc}) + \frac{2}{\alpha} \dots \dots \dots (2) \end{aligned}$$

During step descent, the pitch angle θ_{desc} is negative; therefore, its opposite is used in Eq. (2). Its value can be calculated by means of the geometrical scheme of **Fig. 8**, obtaining the following expression:

$$\begin{aligned} (\gamma + \xi_l) \sin(-\theta_{desc}) + (\beta - 1 - \psi_l) \cos(-\theta_{desc}) \\ + \gamma - \frac{2}{\alpha} - \beta = 0 \dots \dots \dots (3) \end{aligned}$$

which can be solved in $-\theta_{desc}$:

$$\begin{aligned} -\theta_{desc} &= 2 \arctan\left(\frac{N_2}{D_2}\right) \\ N_2 &= -\gamma - \xi_l + ((\gamma + \xi_l)^2 \\ &\quad + \frac{2}{\alpha} \left(-2\beta - \frac{2}{\alpha} + 2\gamma\right) \\ &\quad + 2\beta(-1 - \psi_l + \gamma) + \psi_l(2 + \psi_l) + 1 - \gamma^2)^{\frac{1}{2}} \\ D_2 &= 1 + \psi_l - 2\beta + \gamma - \frac{2}{\alpha} \dots \dots \dots (4) \end{aligned}$$

The static stability condition is verified if the vertical projection of G lies behind the vertical projection of O_l , that is $\lambda_{G,desc} > 0$.

Figures 9 and **10** show the influence of the COM vertical coordinate (ψ_G) and of the step height ($1/\alpha$) on the angle $\lambda_{G,desc}$. Considering the geometry of **Fig. 8**, varying the step height with fixed leg length determines a circular trajectory of G around O_l . Therefore, if the COM is lower than O_l the angle $\lambda_{G,desc}$ has a maximum as a function of ($1/\alpha$), otherwise it decreases monotonically (**Fig. 10**). However, high COM is critical for stability. On the other hand, the effects of the leg length (**Fig. 11**) and of the wheelbase (**Fig. 12**) are less critical during step descent.

Let us note that the range of normalized step height considered in the graphs during step descent is wider than during step ascent, in which there is a stricter limitation, because the rear wheels have to touch the ground when

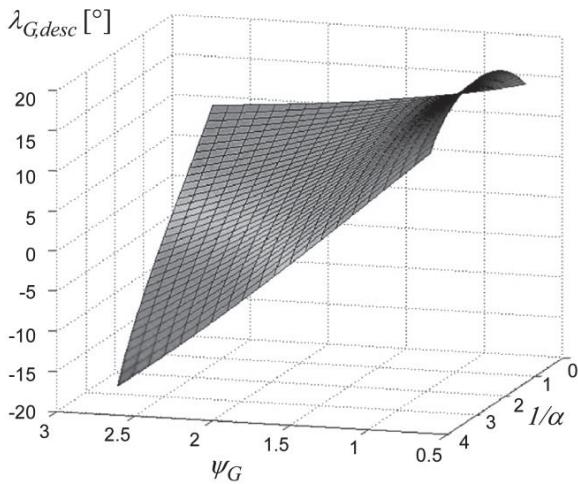


Fig. 9. $\lambda_{G,desc}$ as a function of $1/\alpha$ and ψ_G .

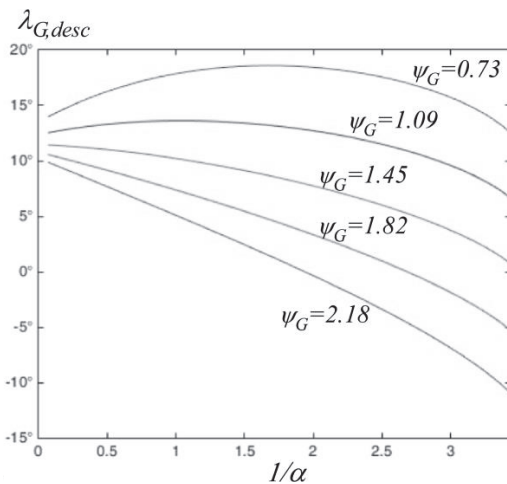


Fig. 10. $\lambda_{G,desc}$ as a function of $1/\alpha$.

the legs are vertical and in contact with the step upper surface [22].

3.3. Experimental Tests on Step Ascent and Descent

Experimental tests have been performed by varying the leg length, wheelbase, and payload position on the Mantis 2 prototype (Fig. 13). While the approximation of quasi-static conditions is fully acceptable during step ascent, which is performed at low speed with the legs always in contact with the ground, during step descent the dynamic effects are more relevant, owing to the impact of the leg tips on the ground. Therefore, while during step ascent, the experimental tests confirm the analytical limit, as discussed in [22], and a $\lambda_{G,asc}$ greater than 5° can be considered a sufficient margin during robot operation, during descent a wider margin is preferable ($\lambda_{G,desc} > 10^\circ$).

4. Hybrid Locomotion Experimental Tests

On uneven terrains and obstacles, Mantis can perform hybrid locomotion, using legs and wheels in combination

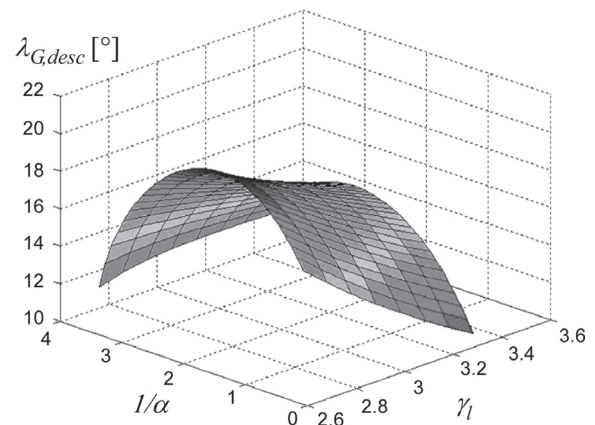


Fig. 11. $\lambda_{G,desc}$ as a function of $1/\alpha$ and γ .

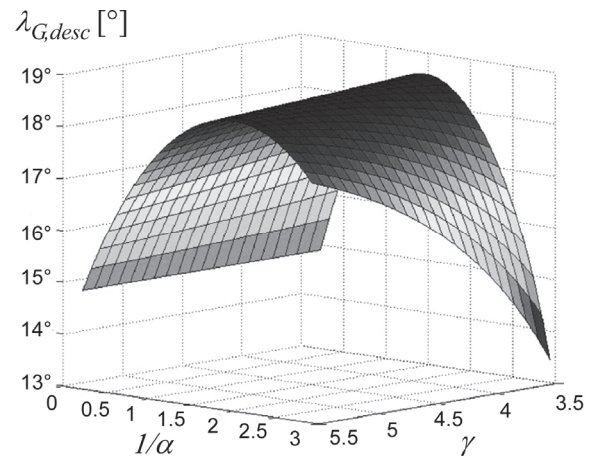


Fig. 12. $\lambda_{G,desc}$ as a function of $1/\alpha$ and γ .

to improve traction. Fig. 14 shows the effectiveness of hybrid locomotion while overcoming some tree roots. As in unstructured environments the obstacle configurations are very variable, it is difficult to measure the influence of the geometrical parameters exhaustively on the hybrid locomotion capability.

In order to solve this problem and to optimize the Mantis' design, also considering the hybrid locomotion capability, a standard test layout has been conceived and built. It is based on a ramp with the z -profile of Fig. 15. The ramp is realized in wood and the static and dynamic friction coefficients between the ramp surface and the robot front wheels and legs have been experimentally measured; their values are respectively around 1.1 and 1.0. The slope of the ramp (angle θ_{ramp} , Fig. 15) is variable; the maximum angle θ_{ramp} that can be climbed in hybrid locomotion for a given set of geometrical parameters is used as measurement of the hybrid locomotion effectiveness. The size of the ramp steps (90 mm) has been selected to highlight the hybrid locomotion effectiveness. As a matter of fact, in case of a z -profile with smaller steps (with size up to approximately 30 mm) the leg action is not necessary, and wheeled locomotion is sufficient.

With this step size, for small angles θ_{ramp} the test is similar to typical hybrid locomotion conditions on un-

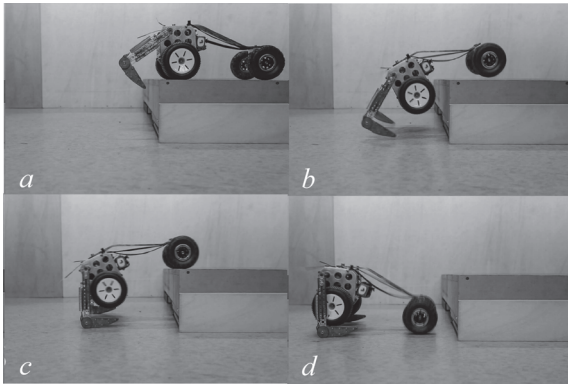


Fig. 13. Experimental tests on the step descent.

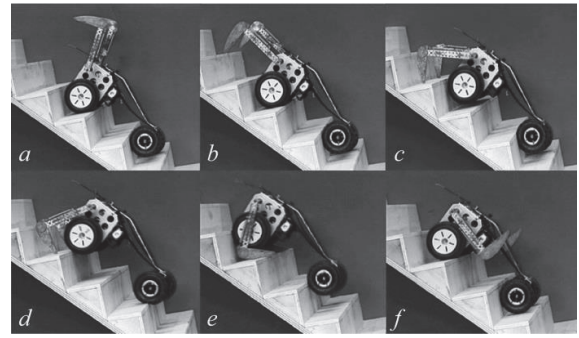


Fig. 16. Hybrid locomotion test.

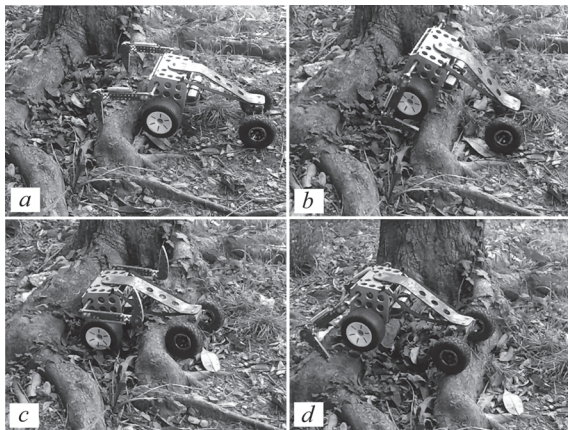


Fig. 14. Hybrid locomotion on uneven terrain.

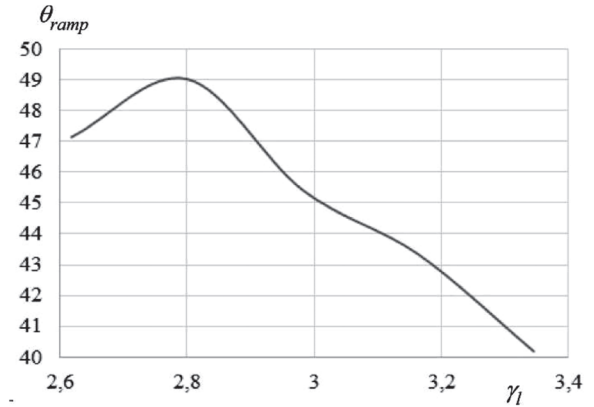


Fig. 17. Maximum angle θ_{ramp} as function of γ_l .

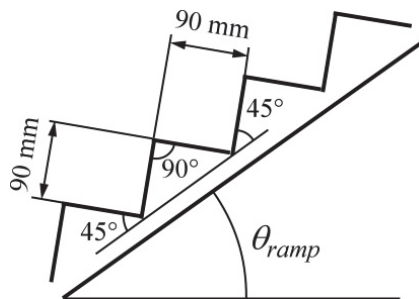


Fig. 15. Z-profile of the hybrid locomotion test ramp.

even ground (Fig. 14); on the other hand, for larger angles the test condition becomes similar to stair climbing with small rise and going.

The most important geometrical ratio for hybrid locomotion on uneven surfaces is the leg length (γ_l). First, hybrid locomotion is possible only if the legs are sufficiently long to touch the ground when the front and rear wheel are in contact with a flat surface; this condition is represented nondimensionally by the following inequality:

$$\gamma_l > \psi_l + 1 \quad \dots \dots \dots (5)$$

Figure 16 represents a hybrid locomotion test on the ramp of Fig. 15, and Fig. 17 represents the maximum angle (θ_{ramp}) which can be climbed as a function of the normalized leg length γ_l . With the base value $\psi_l = 1.45$, the

minimum value of (γ_l) is 2.45, and a better hybrid locomotion performance is obtained with $\gamma_l \cong 2.8$ (Fig. 17). Nevertheless, this value is too low for square step climbing: for $\gamma_l < 2.9$, the final phase of the step ascent cannot be completed correctly. When the front wheels touch the step upper surface, the robot COM, G , is behind the contact point, C , between the auxiliary wheels and the step (Fig. 18, a), so when the legs rotate backward they cannot lift up the rear axle (Fig. 18, b – d). On the other hand, high values of γ_l are critical for stability in step ascent (see Fig. 6). Considering these conflicting requirements, a suitable compromise is in the range of $2.95 < \gamma_l < 3.0$.

5. Conclusion

In the present paper, new analytical and experimental results on the Mantis robot family are discussed. The effects of the main geometrical ratios on stability during square step ascent and descent have been studied analytically, in particular, the normalized leg length γ_l , the normalized wheelbase γ , and the normalized vertical position of the robot COM ψ_G (influenced by the payload). Experimental tests have been performed to estimate proper stability margins during operation, in terms of angles $\lambda_{G,asc}$ and $\lambda_{G,desc}$.

Moreover, a repeatable test ramp with z-profile has been used in order to measure the effectiveness of hybrid

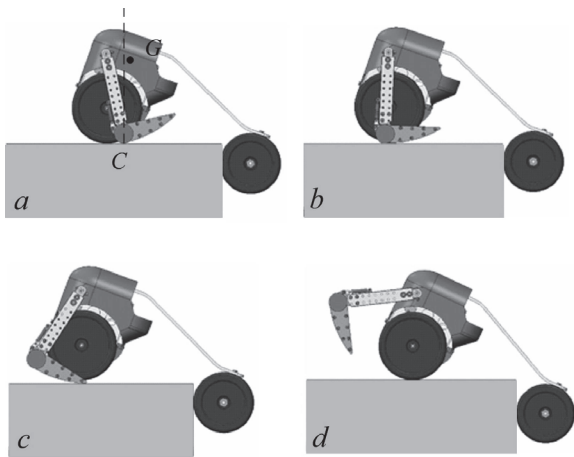


Fig. 18. Step climbing failure caused by too low γ .

locomotion with legs and wheels acting in combination.

The discussed experimental and analytical results show that leg length and wheelbase have to be selected to reach a compromise between conflicting requirements (stability, maneuverability, hybrid locomotion capability). Moreover, if it is necessary to climb not only a single square step but also a stair with multiple steps, the maximum wheelbase is limited by the going of the stair.

In general, the experimental campaign on Mantis 2 has given clear design indications and confirmed the effectiveness of the legs equipped with auxiliary wheels, which were not present in the first version. The tests confirm that the auxiliary wheels improve the reliability of the final phase of step climbing, when the rear axle is lifted by the legs, while traction in hybrid locomotion is unaffected, because they can't rotate backward thanks to the one-way bearings.

The main advantage of the Mantis with respect to other small-scale ground mobile robots is its capability of overcoming steps higher than the robot itself (with the legs pointing backward, in rest position); other important features are the effectiveness of the hybrid locomotion on irregular terrains and obstacles and the purely wheeled locomotion on flat grounds, with high maneuverability and stable camera vision.

There are different topics that will be investigated in the continuation of the research. First, a re-design will be implemented for possible industrial production: a lighter construction with simplified mechanics and use of plastic parts would be preferable to reduce costs. For example, a component that can be remarkably simplified is the leg, adopting a flexure hinge to replace both the passive revolute joint lpj and the spring g (Fig. 1). Another important research direction is the development of an autonomous navigation system, including a control algorithm capable of leg-wheel coordination to improve the dynamic performance during obstacle climbing and descending.

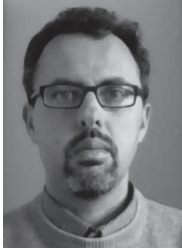
References:

- [1] R. R. Murphy, "Rescue Robotics for Homeland Security," Communications of the ACM – Homeland Security, Vol.47, No.3, pp. 66-

68, 2004.

- [2] R. Playter, M. Buehler, and M. Raibert, "Bigdog," Proc. of the SPIE Defense & Security Symp., Unmanned Systems Technology, 2006.
- [3] E. Semsch, M. Jakob, D. Pavlicek, and M. Pechoucek, "Autonomous UAV Surveillance in Complex Urban Environments," IEEE/WIC/ACM Intl. Joint Conf. on Web Intelligence and Intelligent Agent Technologies (WI-IAT'09), Vol.2, pp. 82-85, 2009.
- [4] E. Cetinsoy, "Design and Flight Tests of a Holonomic Quadrotor UAV with Sub-Rotor Control Surfaces," 2013 IEEE Intl. Conf. on Mechatronics and Automation, pp. 1197-1202, 2013.
- [5] M. Ikeda, S. Hikasa, K. Watanabe, and I. Nagai, "Motion Analysis of a Manta Robot for Underwater Exploration by Propulsive Experiments and the Design of Central Pattern Generator," Int. J. Automation Technol., Vol.8, No.2, pp. 231-237, 2014.
- [6] K. D. Le, H. D. Nguyen, and D. Ranmuthugala, "Development and Control of a Low-Cost, Three-Thruster, Remotely Operated Underwater Vehicle," Int. J. Automation Technol., Vol.9, No.1, pp. 67-75, 2015.
- [7] K. Kato, H. Seki, and M. Hikizu, "3-D Obstacle Detection Using Laser Range Finder with Polygonal Mirror for Powered Wheelchair," Int. J. Automation Technol., Vol.9, No.4, pp. 373-380, 2015.
- [8] Y. Zhuang, N. Jiang, H. Hu, and F. Yan, "3-D-Laser-Based Scene Measurement and Place Recognition for Mobile Robots in Dynamic Indoor Environments," IEEE Trans. on Instrumentation and Measurement, Vol.62, No.2, pp. 438-450, 2013.
- [9] J. Neves, F. Narducci, S. Barra, and H. Y. Proença, "Biometric recognition in surveillance scenarios: a survey," Artificial Intelligence Review, 22 March, pp. 1-27, 2016.
- [10] R. Siegwart and I. R. Nourbakhsh, Introduction to Autonomous Mobile Robots, Cambridge, MA: MIT Press, 2011.
- [11] A. Seeni, B. Schafer, B. Rebele, and N. Tolyarenko, "Robot Mobility Concepts for Extraterrestrial Surface Exploration," Proc. of the IEEE Aerospace Conf., 2008.
- [12] L. Bruzzone and G. Quaglia, "Locomotion Systems for Ground Mobile Robots in Unstructured Environments," Mechanical Sciences, Vol.3, pp. 49-62, 2012.
- [13] R. Altendorfer, N. Moore, H. Komsuoglu, M. Buehler, H. B. Jr. Brown, D. McMordie, U. Saranli, R. Full, and D. E. Koditschek, "RHEx: a biologically inspired hexapod runner," Auton. Robot., Vol.11, No.3, pp. 207-213, 2001.
- [14] R. D. Quinn, G. M. Nelson, R. J. Bachmann, D. A. Kingsley, J. T. Offi, T. J. Allen, and R. E. Ritzmann, "Parallel Complementary Strategies for Implementing Biological Principles into Mobile Robots," Intl. J. Robot. Res., Vol.22, No.3, pp. 169-186, 2003.
- [15] S. D. Herbert, A. Drenner, and N. Papanikolopoulos, "Loper: A Quadruped-Hybrid Stair Climbing Robot," Proc. 2008 IEEE Conf. on Robotics and Automation, Pasadena, CA, May 19-23, 2008.
- [16] R. Siegwart, M. Lauria, P. A. Maesuli, and M. Van Winnendael, "Design and Implementation of an Innovative Micro Rover," Proc. of Robotics 98, 3rd Conf. and Exposition on Robotics in Challenging Environments, 1998.
- [17] G. Quaglia, L. Bruzzone, R. Oderio, and R. Razzoli, "Epi. Q Mobile Robots Family," Proc. of the ASME 2011 Int. Mechanical Engineering Congress & Exposition IMECE2011, Denver, CO, November 11-17, 2011, Vol.7, pp. 1165-1172, 2011.
- [18] G. Quaglia, R. Oderio, L. Bruzzone, and R. Razzoli, "A Modular Approach for a Family of Ground Mobile Robots," Int. J. of Advanced Robotic Systems, Vol.10, 2013.
- [19] K. J. Huang, S. C. Chen, Y. C. Chou, S.-Y. Shen, C.-H. Li, and P.-C. Lin, "Experimental Validation of a Leg-wheel Hybrid Mobile Robot Quattroped," 2011 IEEE Int. Conf. on Robotics and Automation, May 9-13, Shanghai, China, pp. 2976-2977, 2011.
- [20] Y.-S. Kim, G.-P. Jung, H. Kim, K.-J. Cho, and C.-N. Chu, "Wheel Transformer: A Wheel-Leg Hybrid Robot With Passive Transformable Wheels," IEEE Trans. on Robotics, Vol.30, No.6, pp. 1487-1498, 2014.
- [21] J.-J. Chou and L.-S. Yang, "Innovative Design of a Claw-Wheel Transformable Robot," 2013 IEEE Int. Conf. on Robotics and Automation (ICRA), Karlsruhe, Germany, May 6-10, pp. 1337-1342, 2013.
- [22] L. Bruzzone and P. Fanghella, "Mantis: Hybrid Leg-Wheel Ground Mobile Robot," Industrial Robot, Vol.41, No.1, pp. 26-36, 2014.
- [23] L. Bruzzone and P. Fanghella, "Multibody Simulation of the Dynamic Behaviour of a Hybrid Leg-Wheel Ground Mobile Robot," Proc. of the 33rd IASTED Int. Conf. on Modelling, Identification and Control MIC 2014, February 17-19, Innsbruck, Austria, pp. 237-243, 2014.
- [24] L. Bruzzone and P. Fanghella, "Mantis Hybrid Leg-Wheel Robot: Stability Analysis and Motion Law Synthesis for Step Climbing," Proc. of MESA 2014, 10th IEEE/ASME Int. Conf. on Mechatronic and Embedded Systems and Applications, September 10-12, Senigallia, Ancona, Italy, 2014.

- [25] L. Bruzzone and P. Fanghella, "Functional Redesign of Mantis 2.0, a Hybrid Leg-Wheel Robot for Surveillance and Inspection," J. of Intelligent & Robotic Systems, Vol.81, pp. 215-230, 2016.



Name:
Luca Bruzzone

Affiliation:
Assistant Professor, DIME Department, University of Genoa

Address:

Via Opera Pia 15A, 16145 Genova (GE), Italy

Brief Biographical History:

1997 Received his Master degree, magna cum laude, in Mechanical Engineering at the University of Genoa
1999- Assistant Professor of Mechanics of Machinery at the University of Genoa

Main Works:

- L. Bruzzone and G. Quaglia, "Review article: locomotion systems for ground mobile robots in unstructured environments," Mechanical Sciences, ISSN: 2191-9151, eISSN: 2191-916X, Vol.3, No.2, pp. 49-62, 2012.
- G. Quaglia, L. Bruzzone, G. Bozzini, R. Oderio, and R. P. Razzoli, "Epi.q-TG: mobile robot for surveillance," Industrial Robot: An Int. J., Vol.38, No.3, pp. 282-291, ISSN 0143-991X, 2011.
- His research interest is focused on mechanics and control of robots and automation devices.

Membership in Academic Societies:

- International Federation for the Promotion of Mechanism and Machine Science (IFTToMM) Italy



Name:
Giuseppe Quaglia

Affiliation:
Associate Professor, Politecnico di Torino

Address:

Corso Duca degli Abruzzi 24, 10129 Torino, Italy

Brief Biographical History:

1989 Received his Master Degree in Mechanical Engineering from the Politecnico di Torino
1993 Received the Ph.D. in Applied Mechanics, Mechanical System and Structures from the Politecnico di Torino
1994- Researcher and then Professor at Politecnico di Torino

Main Works:

- G. Quaglia and M. Sorli, "Air Suspension Dimensionless Analysis and Design Procedure," Vehicle System Dynamics, Vol.35, No.6, pp. 443-475, 2001.
- G. Quaglia, D. Maffiodo, and F. Pescarmona, "A Novel Continuous Alternate Motion Mechanism With Two Input Wheels," J. of Mechanical Design, ISSN 1050-0472, Vol.129 pp. 858-864, 2007.
- His main fields of research are Robotics, Mechatronics, Systems Dynamic, Mechanisms, Industrial Automation and Technologies for sustainable Human development.

Membership in Academic Societies:

- International Federation for the Promotion of Mechanism and Machine Science (IFTToMM)
- The American Society of Mechanical Engineering (ASME)



Name:
Pietro Fanghella

Affiliation:
Professor, DIME Department, University of Genoa

Address:

Via Opera Pia 15A, 16145 Genova, Italy

Brief Biographical History:

2000- Full Professor of Mechanics of Machines at the University of Genoa
2010- Coordinator of Mechatronic Engineering Laurea Degree at University of Genoa

Main Works:

- His research interest is focused on the kinematics, dynamics and control of mechanical systems and robot, education in mechanical engineering, non-conventional mechanical transmissions.

Membership in Academic Societies:

- Technical Committee on Computational Kinematics, International Federation for the Promotion of Mechanism and Machine Science (IFTToMM)
- Permanent Committee on Education, IFTToMM